

PCCP

Accepted Manuscript



This is an *Accepted Manuscript*, which has been through the Royal Society of Chemistry peer review process and has been accepted for publication.

Accepted Manuscripts are published online shortly after acceptance, before technical editing, formatting and proof reading. Using this free service, authors can make their results available to the community, in citable form, before we publish the edited article. We will replace this *Accepted Manuscript* with the edited and formatted *Advance Article* as soon as it is available.

You can find more information about *Accepted Manuscripts* in the [Information for Authors](#).

Please note that technical editing may introduce minor changes to the text and/or graphics, which may alter content. The journal's standard [Terms & Conditions](#) and the [Ethical guidelines](#) still apply. In no event shall the Royal Society of Chemistry be held responsible for any errors or omissions in this *Accepted Manuscript* or any consequences arising from the use of any information it contains.

Can far-IR action spectroscopy combined with BOMD simulations be conformation selective?

Jérôme Mahé,^{a†} Sander Jaeqx,^{b†} Anouk M. Rijs,^{*b} and Marie-Pierre Gaigeot^{*ac}

Received Xth XXXXXXXXXXXX 20XX, Accepted Xth XXXXXXXXXXXX 20XX

First published on the web Xth XXXXXXXXXXXX 200X

DOI: 10.1039/b000000x

The combination of conformation selective far-IR/UV double resonance spectroscopy with Born Oppenheimer Molecular Dynamics (BOMD) simulations is presented here for the structural characterization of the Ac-Phe-Pro-NH₂ peptide in the far-infrared spectral domain, i.e. for radiation below 800 cm⁻¹. Two conformers have been shown to be present in the experiment, namely a conformer with a γ -turn fold (C7 interaction) and a β -turn fold (C10 interaction). The combined experimental and theoretical work presented here aims to provide spectral features typical of each conformer in this far-IR domain. The simulated BOMD far-IR spectra agree well with the experimental spectra and allow direct assignment of the observed bands. These assignments show that the 400-550 cm⁻¹ spectral domain is conformer selective, allowing to distinguish the H-Bond signature of the γ -turn from the β -turn.

1 Introduction

Understanding the forces that govern the complex protein folding process is one of the holy grails in modern biophysical science¹. One way to obtain insights in this process is to study the folding propensities of small isolated peptides by observing the emergence of secondary structures through intramolecular hydrogen bonding². Conformation-selective mid-IR spectroscopy in combination with harmonic density functional theory (DFT) calculations has proven to be a powerful tool to this end, and is nowadays applied on a routine-basis³⁻⁶. The far-IR region (radiation < 800 cm⁻¹) has often been ignored, due to the possible deficiencies of theoretical tools needed to interpret the experimental spectra in this domain⁷⁻⁹. This far-IR regime not only complements the mid-IR one, but also yields information that is not accessible in the mid-IR. The mid-IR region mostly probes localized structural information, due to the localized character of the vibrations found in this region, such as the structurally diagnostic amide A (NH stretch vibration), Amide I (C=O stretch vibration) and Amide II (NH in-plane-bending vibration) modes of peptides. On the other hand, the far-IR region is characterized by large-scale delocalized vibrations. These vibrations are expected to contain detailed structural information on the

overall structure and are therefore directly diagnostic to various backbone conformations¹⁰⁻¹². Since these vibrations often extend over a large part of the peptide backbone, such delocalized modes are also expected to be important for the dynamical and flexible nature of proteins¹³. Additionally, intrinsic hydrogen bond vibrations can be directly probed in the far-IR region^{14,15}, as previously shown for condensed phase systems using low-frequency FTIR spectroscopy^{16,17}. In contrast, the mid-IR region can indirectly probe hydrogen bonds through frequency shifts of the Amide vibrations. One more advantage of far-IR probing is the possibility to probe larger and more complex molecules. For such molecular systems, the mid-IR region is often spectrally congested due to many overlapping Amide bands and thereby limiting the conformational assignment to families rather than to one specific conformation^{4,18,19}. In these cases the far-IR spectra often still show resolved absorption bands. This is a consequence of the bandwidth of the free electron laser used in these experiments, which is proportional to the output photon energy²⁰.

Synergy between experiments and theoretical calculations is essential to obtain structural information from these low-frequency motions. Static harmonic DFT calculations are known to be insufficient to achieve this task. In a previously published paper²¹, we have shown that Born-Oppenheimer Molecular Dynamics (BOMD) is able to reproduce the far-IR absorption spectra of gas phase peptides, and can therefore be employed to obtain structural information from the far-IR absorption region of peptides. This combination is able to distinguish between subtle differences in peptide conformations, superior to static DFT calculations in combination with mid-IR spectroscopy. For example, far-IR spectroscopy coupled with

^a LAMBE CNRS UMR8587, Université d'Evry val d'Essonne, Blvd F. Mitterrand, Bât Maupertuis, 91025 Evry, France

^b Radboud University, Institute for Molecules and Materials, FELIX Laboratory, Toernooiveld 7c, 6525 ED Nijmegen, The Netherlands, E-mail: a.rijs@science.ru.nl

^c Institut Universitaire de France, 103 Blvd St Michel, 75005 Paris, France, E-mail: mgaigeot@univ-evry.fr

†J.M and S.J have equally contributed to the work

BOMD simulations could differentiate the axial and equatorial forms of the γ -turn interaction in Ac-Phe-Gly-NH₂, which was not possible with mid-IR spectroscopy and static (harmonic) DFT calculations^{22,23}. As will be described in the present paper, BOMD simulations take the anharmonic character of the delocalized vibrations directly into account, providing reliable spectroscopic predictions, vibrational assignments and structural interpretations. The combination between experiment and theory provides direct insight in the nature of the low frequency motions.

Apart from our developed far-IR set-up for the investigation of neutral gas phase peptides using the FELIX Free Electron Laser²¹, such spectroscopy has been developed in the Havenith group with investigations specifically focused on the probing of the solvation of biomolecules, see for instance refs.^{24–26}. In the groups of Plusquellic and Markelz, terahertz studies are performed on condensed phase biological systems, from simple amino acids to complete proteins.^{10,14} Far-IR spectra of tagged gas phase ionic clusters have also been obtained by the Asmis group in Berlin, see their review²⁷. Protonated clusters and ionic clusters of atmospheric interest have mainly been investigated with this technique. Lastly, far-IR studies are employed to study the structural properties of metal clusters²⁸.

As yet, the far-IR part of the absorption spectrum of gas phase peptides is in many aspects uncharted territory. To identify the functional vibrations and distinguish them from other bands in the spectrum demands a large understanding of the low frequency modes. We have started such mapping in ref.²¹ by combining far-IR experiments and BOMD simulations, and we continue this approach here with Ac-Phe-Pro-NH₂ to assess the conformation selectivity capabilities of our approach. Previous experiments on Ac-Phe-Pro-NH₂ performed in the 3 micron region (probing the NH stretch vibrations) by Mons et al.²⁹ have shown that the backbone of this peptide can fold either via a β -turn (the backbone adopts a C10 interaction, with an unusual cis conformation for the Phe-Pro peptide bond) or a γ -turn (the backbone exhibits a C5 and C7 interaction). These two conformations co-exist in the molecular beam expansion experiments. Choosing this specific peptide allows us to directly observe the difference between backbone folding, here between the C10 and C7 interactions, in far-IR patterns. In that respect, going from Ac-Phe-Gly-NH₂ and Ac-Phe-Ala-NH₂ (previous work²¹, axial and equatorial C7 γ -turns), to Ac-Phe-Pro-NH₂ (present work, C7/C10 H-Bond folding), provides the opportunity to probe different structural motifs which signatures are identified through far-IR and BOMD vibrational spectroscopy.

2 Methods

2.1 Experimental details

Ac-Phe-Pro-NH₂ (95 % purity) was purchased from Genecust (Dudelange, Luxembourg) and used without further purification. Here, the experimental set-up is briefly described. A complete description of the set-up is described elsewhere³⁰. The sample was mixed with graphite powder and applied on a solid graphite bar. A pulsed YAG laser operating at 1064 nm (Polaris Pulsed Nd:YAG Laser, NewWave Research) with a pulse energy of about 1.5 mJ was used to desorb the sample molecules from the graphite substrate as intact neutral molecules. The gas-phase molecules are entrained in a supersonic molecular beam of argon, produced by a pulsed valve (Jordan) and a backing pressure of 3 bar of Argon. In the molecular beam, the peptide molecules are cooled towards their rotational and vibrational ground state³¹. The molecular beam travels through a skimmer about 10 cm downstream to enter a differentially pumped chamber equipped with a reflectron time-of-flight mass spectrometer. Here, the molecules interact with a UV beam produced by a pulsed Nd:YAG laser (either Innolas GmbH Spotlight 1200 or Quanta-Ray Lab Series) coupled to a frequency doubled dye laser (Radiant Dyes NarrowScan, laser dye: coumarin 153). The UV laser was operated at 10 Hz with typical pulse energies of 1 - 2 mJ. The molecules are 2-photon ionized via a one color (1 + 1) REMPI scheme. Conformation selection is achieved by fixing the UV laser at a specific $S_1 \leftarrow S_0$ transition. Since different conformations have a slightly different electronically excited state energy, they will therefore appear as different peaks in the UV excitation spectrum. The generated ions are accelerated into the time-of-flight tube, and reflected into the detector.

For the IR-UV double resonance spectra, the IR and UV beams were spatially overlapped, but the IR pulse precedes the UV pulse by ~ 200 ns. The IR radiation is produced by the Free Electron Laser for Infrared eXperiments (FELIX) located at the FELIX laboratory at the Radboud University²⁰. The frequency of the UV probe pulse is fixed on a transition producing a constant ion signal. For the γ -turn conformation the UV laser was set at 37435.5 cm^{-1} , while at 37409 cm^{-1} for the β -turn conformer (see Figure SI-1 of the supporting information). Whenever the IR hole-burn laser excites a transition that shares the same ground state as the probe laser (and thus is the same conformation), a dip in the ion signal is observed since the ground state is depleted by the IR laser. An IR absorption spectrum of a single conformer can thus be constructed by taking the logarithm of the ion signal without the IR pulse divided by the ion signal with IR pulse. To correct for long-term UV power drifts and changing source conditions, alternating IR-on and IR-off signals are measured by operating the IR laser at 5 Hz and the UV laser at 10 Hz. Since the experiments are

performed over a very wide frequency range, the IR laser intensity needs to be corrected for the photon energy. A photon flux resulting in a 1 mJ pulse energy at 1000 cm^{-1} is equal to a photon flux resulting in a 0.1 mJ pulse energy at 100 cm^{-1} , assuming that the laser pulse profile is identical at the two photon energies. Therefore, the observed absorption intensities are multiplied with the photon energy (in wavenumbers) and renormalized to correct for this effect.

2.2 Theoretical details

Our theoretical methodology consists in DFT-based molecular dynamics simulations, performed within the Born-Oppenheimer (BOMD) framework using the CP2K package^{32,33}. The methods and algorithms employed in the CP2K package are described in detail in ref.³². In our dynamics, the nuclei are treated classically and the electrons quantum mechanically within the DFT formalism. Dynamics consist of solving Newton's equations of motion at a finite temperature, with the forces that act on the nuclei derived from the Kohn-Sham energy. In BOMD, the Schrödinger equation for the electronic configuration of the system is solved at each time step of the dynamics. Mixed plane waves and gaussian basis sets are used in CP2K. Only the valence electrons are taken into account and pseudo-potentials of the Goedecker-Tetter-Hutter (GTH) form are used³⁴⁻³⁶. We use the Becke, Lee, Yang and Parr (BLYP) gradient-corrected functional^{37,38} for the exchange and correlation terms. Dispersion interactions have been included with the Grimme D3 corrections³⁹. Calculations are restricted to the Γ point of the Brillouin zone. We employed plane-wave basis sets with a kinetic energy cut-off of 450 Ry and gaussian basis sets of aug-TZV2P type. The cubic box size is 20 Å length. The kinetic energy cut-off, basis set size and cubic box size have been selected subsequent to energy convergence tests.

The first 3 ps of the trajectory was used for the thermalisation of the system with temperature control through velocity rescaling. Hereafter, pure NVE trajectories were accumulated over 20 ps for the IR spectra calculations and trajectory analyses. Periodic boundary conditions were applied (neutral molecule). The time step in the simulations is 0.4 fs. The temperature of the trajectories was $48\pm 4\text{ K}$ and $53\pm 5\text{ K}$, respectively for the γ -turn and β -turn conformers.

Within statistical mechanics and Linear Response Theory^{40,41}, an infrared spectrum can be calculated by the Fourier Transform of the time correlation function of the fluctuating dipole moment vector of the absorbing molecular system:

$$I(\omega) = \frac{2\pi\beta\omega^2}{3cV} \int_{-\infty}^{\infty} dt \langle \delta\mathbf{M}(t) \cdot \delta\mathbf{M}(0) \rangle \exp(i\omega t) \quad (1)$$

where $\beta = 1/kT$, T is the temperature, c is the speed of light in vacuum, V is the volume. The angular brackets represent a

statistical average of the time correlation function of the dipole vector, where $\delta\mathbf{M}(t) = \mathbf{M}(t) - \langle \mathbf{M} \rangle$ with $\langle \mathbf{M} \rangle$ the time average of $\mathbf{M}(t)$. The calculation in equation 1 is done in the absence of an applied external field. For the prefactor in equation 1, we have taken into account an empirical quantum correction factor (multiplying the classical line shape) of the form $\beta\hbar\omega/(1 - \exp(-\beta\hbar\omega))$, which was shown by us and others to give accurate results on calculated IR intensities⁴²⁻⁴⁴. For more detailed discussions on quantum corrections, see for instance refs.⁴⁵⁻⁴⁸.

The main advantages of the molecular dynamics (MD) approach in equation 1 for the calculation of infrared spectra (also called "dynamical spectra" in the remainder of the text) are discussed in detail in our review⁴⁹ and are briefly listed as follows:

- There are no approximations made in equation 1 apart from the hypothesis of linear response theory, i.e. a small perturbation from the applied external electric field on the absorbing molecular system. Such condition is always fulfilled in vibrational spectroscopy of interest here. There are no harmonic approximations made, be they on the potential energy surface or on the dipole moment, contrary to the usual static calculations used in the literature. These approximations are not needed in equation 1.

- As a consequence, vibrational anharmonicities are naturally taken into account in equation 1: one thus only needs the knowledge of the time evolution of the dipole moment of the system in order to calculate an anharmonic IR spectrum. This is naturally achieved with molecular dynamics simulations. In fact, the finite temperature dynamics takes place on all accessible parts of the potential energy surface, be they harmonic or anharmonic. The quality of the potential energy surface is entirely contained in the "ab-initio" force field used in the dynamics, calculated at the DFT/BLYP+dispersion level in the work presented here. The good to excellent agreements of the absolute (and relative) positions of the different active bands obtained in our theoretical works (see for instance dynamical spectra in the gas phase⁵⁰⁻⁵⁴, in the liquid phase^{42,55-58}, and at solid-liquid and liquid-air interfaces⁵⁹⁻⁶¹) is a demonstration that this level of theory is correct.

- Crucial to the present discussion, the calculation of IR spectra with MD is related *only* to the time-dependent dipole moment of the molecular system, neither requiring any harmonic expansion of the transition dipole moment nor the knowledge of normal modes, in contrast to harmonic calculations. Therefore, if the dipole moments and their fluctuations are accurately calculated along the trajectory, the resulting IR spectrum should be reliable. The vibrations therefore do not directly rely on the curvature of the potential energy surface at the minima on the PES (i.e. normal modes and derivatives using these normal modes used in static DFT calculations) but rather on the time evolution of the electric dipole moment of

the molecular system, which is governed by the conformational dynamics at the finite temperature of the simulation. As a consequence, dynamical anharmonic spectra from equation 1 and harmonic spectra rely on strictly different properties, and presumably require different levels of accuracy for the evaluation of these properties.

- Equation 1 gives the whole infrared spectrum of a molecular system in *one single calculation*, i.e. the band positions, the band intensities and the band shapes, through the Fourier transform of a time correlation function. There are no approximations applied, in particular the shape and broadening of the vibrational bands result from the underlying dynamics and mode-couplings of the system at a given temperature.

No scaling factors of any kind are applied to the vibrations extracted from the dynamics. The sampling of vibrational anharmonicities, i.e. potential energy surface, dipole anharmonicities, mode couplings, anharmonic modes, is included in our simulations, *by construction*, and the application of a scaling factor to the band positions is therefore unnecessary. As reviewed in previous papers, excellent agreements between dynamical spectra and IR-MPD, IR-PD and IR-UV ion dip experiments have been achieved. Any remaining discrepancies between dynamical and experiment spectra should mainly be due to the choice of the DFT/BLYP+dispersion functional as DFT-based dynamics are only as good as the functional itself allows.

The length of the trajectory is related to the vibrational domain to be sampled. One has to keep in mind that the time-length has to be commensurate with the investigated vibrational motions. Hence, trajectories around 5 ps are just enough in order to sample stretching motions in the high frequency domain of 3000-4000 cm^{-1} , provided that several trajectories starting from different initial conformations (structure and/or velocities) are accumulated and averaged for the final IR dynamical spectrum. In the mid-IR domain, trajectories of at least 10 ps each are needed in order to sample the slower stretching and bending motions of the 1000-2000 cm^{-1} domain. In the far-IR below 1000 cm^{-1} of interest to the present work, longer trajectories are needed in order to properly sample the much slower motions typical of that domain, i.e. torsional motions and possibly opening/closure of structures, typical of peptide chains. In Figure 1, we have reported the dynamical IR spectrum of the γ -turn conformer calculated each 5 ps of trajectory over 20 ps, in the critical 100-400 cm^{-1} lower frequency part. One can see that a 20 ps trajectory already allows an excellent convergence of the dynamical IR spectrum (a 100 cm^{-1} is sampled 60 times in that time period).

An accurate calculation of anharmonic infrared spectra is one goal to achieve, the assignment of the active bands into individual atomic displacements or vibrational modes is another one. This issue is essential to the understanding of the

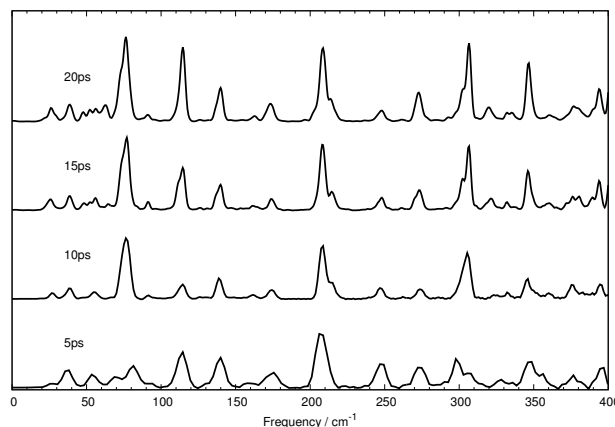


Fig. 1 Dynamical IR spectrum of the γ -turn conformer in the 100-400 cm^{-1} domain, calculated each 5 ps over a 20 ps trajectory, to illustrate the convergence of the spectrum with respect to time-length.

underlying molecular, structural and dynamical properties. In molecular dynamics simulations, the interpretation of the infrared active bands into individual atomic displacements traditionally relies on Fourier transforms of time correlation functions based on velocities or on positions⁴⁹. Because of the intrinsic nature of delocalised and coupled modes in the far-IR spectral range, we have adopted here a strategy of assignments in terms of Fourier transforms of intramolecular coordinates (IC) time correlation functions, named ICDOS in the rest of the paper, following our previous work on far-IR spectra²¹:

$$I_{ICDOS}(\omega) = \int_{-\infty}^{\infty} \langle IC(t) \cdot IC(0) \rangle \exp(i\omega t) dt. \quad (2)$$

Figure 2 provides a scheme of the PhePro molecule together with the labelling of atoms and definitions of dihedral angles discussed below. As the spectral domain $< 1000 \text{ cm}^{-1}$ is related to large amplitude motions, we have chosen intramolecular coordinates such as dihedral angles (from the backbone, see ϕ , ψ and ω in Fig. 2 and table SI-2, from the side chain that carries the Phenyl ring, see χ_1 and χ_2 in Fig. 2), out-of-plane (wagging) motions of H atoms that belong to the Phenyl ring or to the Proline residue (labelled Dihedral-Ring- $H_{x,y,z}$ and Dihedral-Pro- $H_{1,2,3}$ in Fig 5). We have also calculated the vibrational signature of two coordinates directly related to the C10/C7 hydrogen bond motion, the H-Bond stretching defined as the $\text{NH}_2 \cdots \text{O}=\text{C}$ distance, and the dihedral angle $H_{bond}\text{-N-C-C}$ where H_{bond} is the NH_2 atom hydrogen bonded to the $\text{C}=\text{O}$ group. We have also calculated the vibrational signature of the dihedral angle $H_{free}\text{-N-C-C}$ where H_{free} is the free hydrogen atom of the NH_2 group. The signature of the wagging motion of the backbone N-H amide group (labelled Dihedral- H_{phe} in Fig 5) has also been calculated.

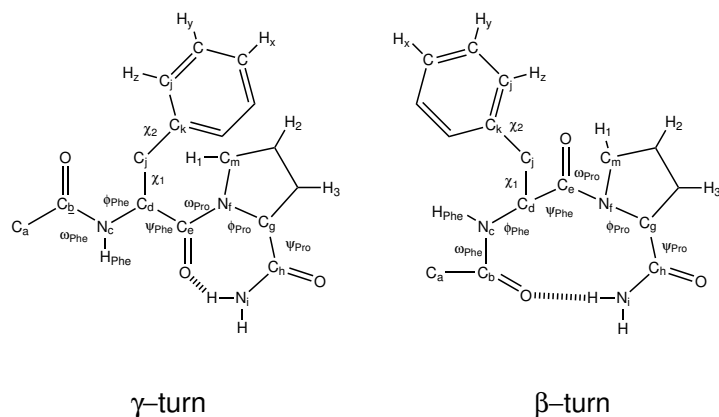


Fig. 2 Scheme of the PhePro molecule with labelling of atom names and dihedral angles (ϕ , ψ , ω and χ) employed in the text for the assignment of the IR features. The angles are defined as follows, see scheme 2: $\phi_{Phe} = (C_e, C_d, N_c, C_b)$, $\psi_{Phe} = (N_f, C_e, C_d, N_c)$, $\omega_{Phe} = (O, C_b, N_c, H_{Phe})$, $\chi_1 = (N_c, C_d, C_j, C_k)$, $\chi_2 = (C_d, C_j, C_k, C_l)$, $\phi_{Pro} = (C_e, N_f, C_g, C_h)$, $\psi_{Pro} = (N_f, C_g, C_h, N_i)$, $\omega_{Pro} = (O, C_e, N_f, C_m)$.

3 Results

3.1 Conformational assignment

The REMPI spectrum of Ac-Phe-Pro-NH₂ is shown in the supplementary information (Figure SI-1). The spectrum closely resembles the one previously measured by Mons *et al.*²⁹ We recorded the IR spectra for the major peaks observed in the spectrum and found two different IR spectra. This suggests that two conformations of Ac-Phe-Pro-NH₂ are present in our molecular beam expansion experiment. Figure 3 shows the IR spectra for the γ -turn (red line) and β -turn (blue line) recorded from 1850 down to 100 cm⁻¹ with the UV frequency fixed at 37435.5 and 37409 cm⁻¹, respectively. Each IR spectrum shows intense bands throughout the complete IR region, and both spectra show many well-resolved features down to the far-IR region where we observed narrow peaks with a FWHM of about 3 cm⁻¹, limited by the bandwidth of the free electron laser.

The mid-IR region is commonly used to identify peptide structure(s). Here, the Amide I region of the γ -turn conformer is composed of three clear peaks between 1780-1610 cm⁻¹, originating from the three backbone C=O stretch modes. In contrast, only two peaks are observed for the β -turn peptide. Here, the three C=O stretching modes lie too close to each other to be resolved. The three C=O stretch frequencies are calculated to differ by around 22 cm⁻¹. Considering a FWHM of 1-2% for the FELIX IR source, it is not surprising that these absorption bands are not fully resolved. The medium intense band observed at about at 1580 cm⁻¹ (γ -turn) and 1600 cm⁻¹ (β -turn) results from the NH₂ scissor

vibration.

The experimental spectrum in red in Figure 3 is readily assigned to the gamma-turn (β - γ_L) conformation of PhePro with the phenyl group in the "a orientation". Here, the " β " does refer to a C5 interaction which are responsible for the formation of β -sheets in protein structures. This is the lowest energy structure found in our conformational search and it has the best match in the 1000-1850 cm⁻¹ region, see Figure SI-2. Mons *et al.* have also assigned the "a phenyl orientation" to the structure based on the Franck-Condon patterns in the REMPI spectrum²⁹.

For the spectrum shown in blue in Figure 3, the assignment is not that straightforward. This spectrum was previously assigned to a type VIa β -turn conformation with a cis conformation of the Phe-Pro peptide bond by Mons *et al.*²⁹. The "VIa" is used to classify different types of β -turn conformations. This is also our conclusion from the present work. However, the orientation of the phenyl ring was not discussed in detail in that paper. We therefore performed geometry optimizations of the three different a, g+ and g- possible orientations of the phenyl group in the β -turn geometry, and we calculated the associated harmonic IR spectra for the mid-IR region (1000-1800 cm⁻¹, with the B3LYP functional) and for the 3 μ m region (2000-4000 cm⁻¹, with the B97-D functional), including mode dependent scaling factors⁶². We also performed BOMD simulations (with the BLYP+D3 functional) in order to get the anharmonic far-IR spectra of these three phenyl ori-

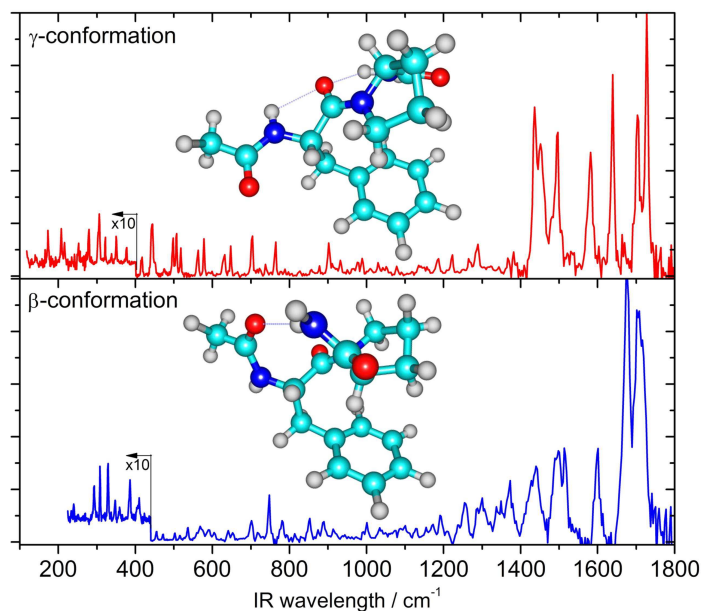


Fig. 3 Recorded IR absorption spectra for the γ -turn (top) and β -turn (bottom) in the range 100 cm⁻¹ - 1850 cm⁻¹ region. The optimized structures of the assigned structures are shown as well.

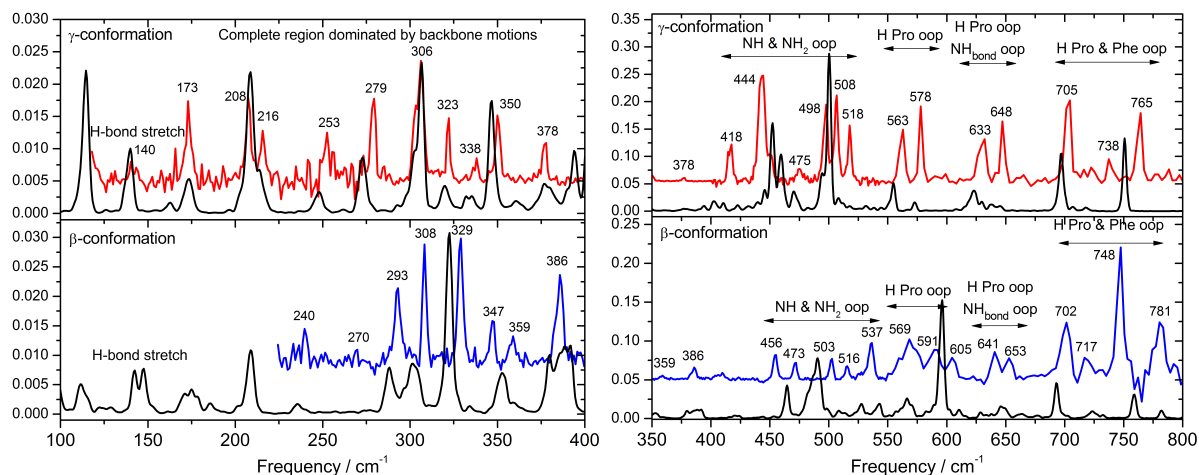


Fig. 4 Comparison between the dynamical BOMD spectra in red and experimental spectra in black in the 100-400 cm^{-1} domain. The position of the H-bond stretching vibration is indicated as well. Comparison between the dynamical BOMD spectra in red and experimental spectra in black in the 400-800 cm^{-1} domain. In the experimental spectra various regions are indicated where the assignment between the two conformations is very similar.

entations in the β -turn geometry of PhePro, see Figure SI-3. The goal is to assign one of these orientations to the experimental spectra. Note that the energies of the a, g+ and g- orientation of the phenyl group in the β -turn optimized structures are 1.22 kcal.mol^{-1} , 3.85 kcal.mol^{-1} and 3.79 kcal.mol^{-1} respectively, using the B97-D/6-311G+(d,p) level of theory (the 0 kcal.mol^{-1} is assigned to a γ -turn structure).

These calculations clearly show that the phenyl group is in its "a orientation", see Figure SI-3, Figure SI-4 and Table SI-1. For discarding the "g+ orientation", the most convincing evidence is found in the 3 μm range. As Table SI-1 shows, in this orientation the NH backbone group of Phe interacts with the phenyl ring, causing a strong red shift for the NH stretch vibration. This shift is not observed in the experimental spectrum. The "g- orientation" can be excluded due to the far too intense absorption peaks in the far-IR at 408 cm^{-1} predicted by the BOMD simulations (Figure SI-3). The "a orientation" also reproduces the peak patterns in the 1000-1400 cm^{-1} range (Figure SI-4).

The assigned γ - and β -turn structures with the "a-orientation" of the phenyl group have been further investigated in our BOMD simulations.

3.2 BOMD spectra

Figure 4 presents the experimental and theoretical IR spectra of the γ -turn (top) and β -turn (bottom) conformers of PhePro in the 100-400 cm^{-1} region and 400-800 cm^{-1} region respectively. Note that the absorption intensity is lower below 400 cm^{-1} and the scales in Figure 4 are adjusted accordingly.

We remind that the dynamical theoretical spectra have not

been adjusted in any way (neither band positions, nor band-widths and shapes). The first observation is that theory and experiment bear remarkable agreement. The theoretical spectra display a number of peaks, positions, band-shapes and intensities that are indeed in good to excellent agreement with the experiments in this anharmonic far-IR frequency range. A few theoretical bands are however too broad in comparison to the experiments and there are also a few bands that either lack intensity or on the contrary carry too much intensity in the theoretical spectra. We will come back to these issues in the discussion. The agreement between experiment and theory is especially remarkable for the γ -turn conformer. The theoretical spectrum of the β -turn shows deficiencies with respect to the experiment, mainly in the higher energy region, that are not observed in the theoretical spectrum of the γ -turn.

One can also observe from the experiments and calculations that the β -turn and γ -turn conformers have different signatures in the 100-800 cm^{-1} domain, thus this region certainly allows us to distinguish both conformers from their IR spectra alone in the far-IR range.

Figure 5 report band assignments of the dynamical IR spectra following the method described in section 2. These assignments are discussed hereafter.

From the experimental and theoretical spectra, one can observe that the 550-800 cm^{-1} IR spectral region does not appear to be very much conformer selective, as the number of peaks and their positions are very similar between the β - and γ -turn conformers. Making a one-to-one comparison of the position of the peaks between the two conformers in this region, the maximum band-shift that can be observed is roughly 16 cm^{-1} , with an average difference in the peak positions be-

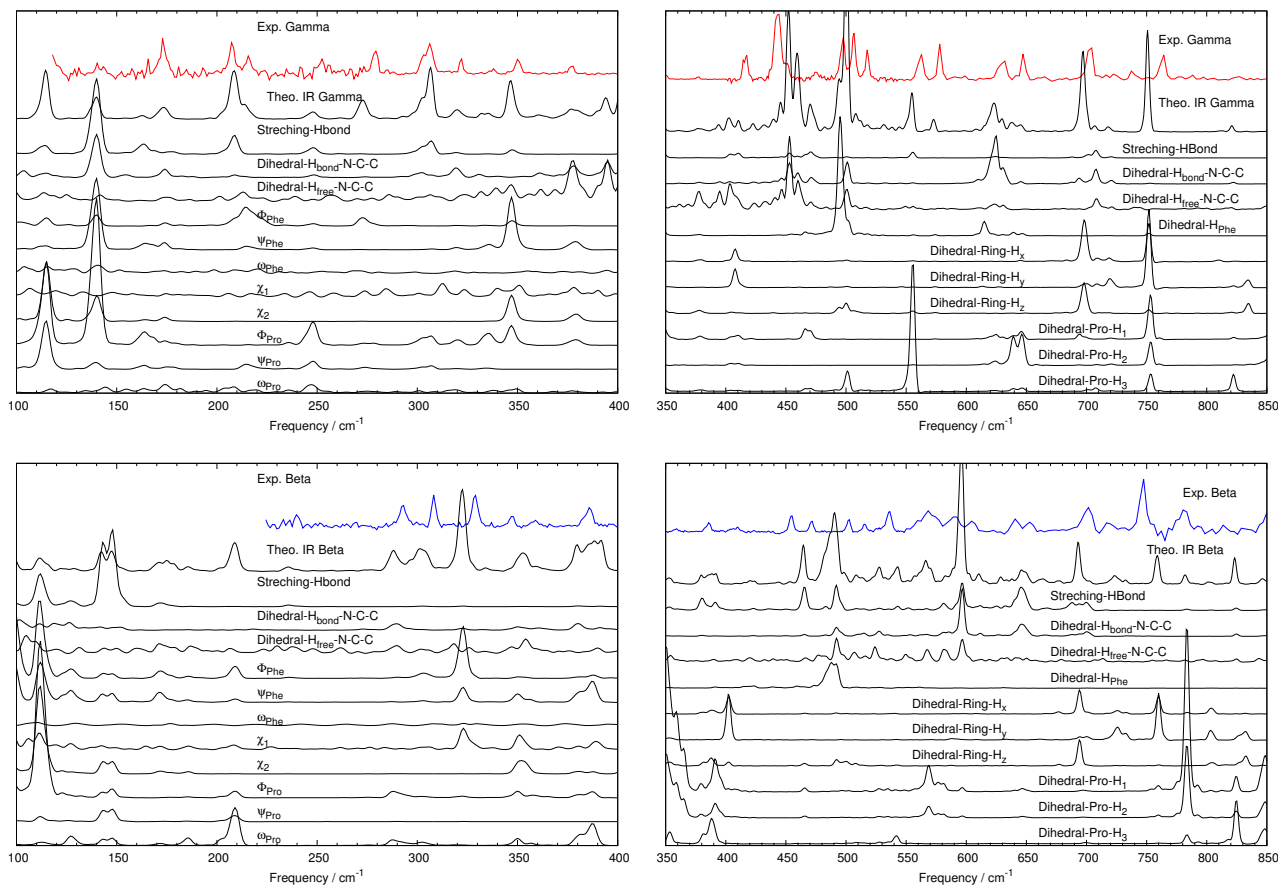


Fig. 5 Decomposition of the vibrational bands of γ -turn conformer (top) and β -turn conformer (bottom) of PhePro in terms of delocalised motions, using ICDOS, the chosen IC are dihedral motions, C7 H-Bond motion and NH₂ free H atom dihedral motion. Dihedrals ϕ , ψ , ω and χ are defined in fig 2. See also eq 2 for the definition of ICDOS.

tween the two conformers of $\sim 7 \text{ cm}^{-1}$.

That this domain does not appear conformer selective can be very well understood by the bands assignments, as we find that the $550\text{-}800 \text{ cm}^{-1}$ bands predominantly arise from out-of-plane wagging motions of H atoms, for both β - and γ -turn conformers of PhePro. These waggings are either due to H atoms that belong to the phenyl ring or H atoms belonging to the proline ring residue. As can be seen in the 3D structures in Figure 3, the two conformers display very similar environments around the Pro and Phe rings, so that one would indeed expect very similar signatures of the H waggings on these two rings, whether they belong to the β - or γ -turn conformers.

The $700\text{-}800 \text{ cm}^{-1}$ domain is hence composed of a mixing of out-of-plane wagging motions of H atoms that belong to the phenyl ring and of H atoms that belong to the Pro ring. The band located at 700 cm^{-1} is on the contrary predominantly arising from the out-of-plane waggings of H atoms that belong to the phenyl ring. One can see that the signatures arising at

705 , 738 and 765 cm^{-1} for the γ turn (702 , 717 and 748 cm^{-1} for the β turn) from H atoms that belong to the phenyl ring were also present in our previous work about PheAla and PheGly systems²¹. These features seem to be specific to the aromatic ring. The peaks located at 648 cm^{-1} for the γ -turn and 641 and 653 cm^{-1} for the β -turn are due to out-of-plane wagging motions of H atoms of the proline residue.

The C10 (β -turn) and C7 (γ -turn) hydrogen bond signature seen through the torsional motion of the H-Bonded hydrogen atom of NH₂ (signature of H_{bond}-N-C-C in fig. 5) is also appearing in this region. It explains the 633 cm^{-1} peak for the γ -turn while this H-Bond signature overlaps with the out-of-plane wagging motions of H atoms of the proline residue for the β -turn conformer. The two thin peaks at 563 and 578 cm^{-1} for the γ -turn conformer and the broader peaks at 569 and 591 cm^{-1} for the β -turn are also due to the out-of-plane wagging motions of H atoms of the proline residue. The participation of the C10 H-Bond is also appearing in these bands for the

β -turn conformer. One peak of the doublet lacks intensity in the dynamical spectrum of the γ -turn conformer, while both peak intensities of the β -turn conformer are underestimated in the dynamical spectrum.

The 400-550 cm^{-1} spectral domain appears conformer selective, providing distinct signatures for the β - and γ -turns, as will be discussed below, although the general spectral features in this domain are similar between the two conformers. Both conformers hence give rise to a triplet between ~ 490 -540 cm^{-1} and to a doublet between ~ 400 -470 cm^{-1} . Note that only the higher frequency band of the triplet (518 cm^{-1} for the γ -turn, 537 cm^{-1} for the β -turn) shows a substantial 19 cm^{-1} upshift when comparing the spectra of the two conformers. On the contrary, the doublet peaks are substantially shifted in position between the two conformers, with the two signatures being upshifted by +38 and +29 cm^{-1} for the β conformer with respect to the γ conformer. It is also interesting to note that all peaks (triplet and doublet) in this domain are substantially more intense in the spectrum of the γ -turn conformer.

For the γ -turn, only a single intense peak is predicted in place of the experimental triplet, although much lower intensity peaks can be seen in the tail of the intense peak, while the triplet is correctly predicted for the β -turn. The doublet of the β -turn from the dynamical spectrum is blue-shifted from experiment. Interestingly, the subtle details of the γ -turn doublet are well predicted in the dynamical spectrum, up to the 475 cm^{-1} tail peak. We find that the triplet and doublet features are due to N-H torsional/out-of-plane motions, whether N-H belongs to the NH_2 function (free and H-bonded N-H signatures in this domain) or to the amide backbone N-H. The triplet in the γ -turn arises from a combination of all N-H signatures, merging into one single peak in the BOMD spectrum, contrary to the experiment. The triplet in the β -turn is on the contrary solely due to the free N-H group of the NH_2 terminus of the peptide. For both β - and γ -turn, the doublet clearly reflects the signature of the free N-H of the NH_2 function, while this signature is also overlapping with the N-H \cdots O H-Bond signature for the β -turn conformer.

The doublet is thus directly (β -turn) / indirectly (γ -turn) related to the C10/C7 hydrogen bond. It is clear from Figure 6 where the evolution with time of the H \cdots O H-Bond of the C10 β -turn (blue line) and of the C7 γ -turn (red line) conformers is reported, that the average H-Bond length and the fluctuations around the average differ between the two conformers (same temperature for the two trajectories). While this H-Bond is 2.01 ± 0.08 Å on average for the γ -turn conformer, it is 1.95 ± 0.09 Å, on average for the β -turn conformer (see Table SI-2). This shows how the C10 ring of the β -turn is more tightly H-Bonded than the C7 ring of the γ -turn. This difference directly reflects the strength of the hydrogen bond, with the C7 γ -turn H-Bond being weaker. With this strength differ-

ence in mind, one is therefore not surprised that the signature of the C7 H-Bond in the γ -turn conformer appears at lower frequencies, and that the C10 has a more direct signature in the doublet assignment than the C7. Experiments and dynamical spectra show that the C10 H-Bond signature is up-shifted from the C7 signature, roughly by ~ 30 -40 cm^{-1} , providing a distinct signature of the γ - versus β -turn for the PhePro peptide.

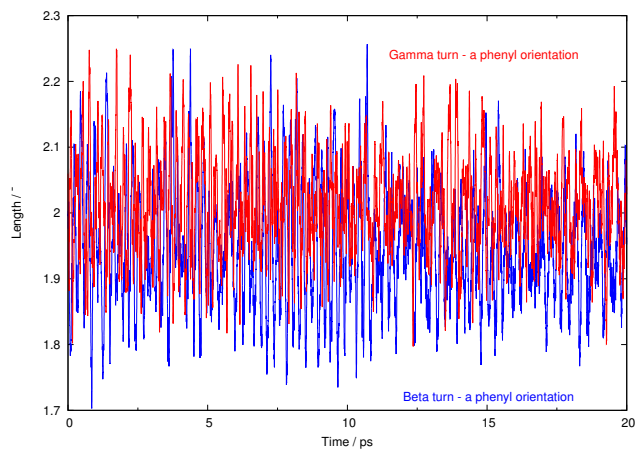


Fig. 6 Evolution with time of the length of the H \cdots O H-Bond in the C10 β -turn (blue line) and in the C7 γ -turn (red line). This is plotted over 20 ps of the trajectories.

One more comment about the weaker C7 H-Bond (γ -turn) with respect to the C10 one (β -turn). It is well-known that GGA functionals such as BLYP underestimate H-Bond strengths, which consequently might allow too large amplitude motions of the hydrogen atoms involved in the hydrogen bond. This subsequently might lead to too large associated vibrational bands, which is indeed observed in the 450-480 cm^{-1} doublet in the dynamical spectrum of the β -conformer. These two bands also have lower intensities in the experimental spectra, showing that our representation presumably overestimates the H-Bond motions in the β -turn C10 interaction. This is also observed for the C7 interaction of the γ -turn, but to a lower extent.

To understand the spectral domain below 400 cm^{-1} , we have used the ICDOs vibrational signatures (Internal Coordinates Density Of States) of backbone torsional motions, of the hydrogen bond and of the out-of-plane motion of H atoms that belong to the NH_2 functional group. This is shown in Figure 5. First of all, out-of-plane motion of the hydrogen atoms that belong to NH_2 function do not seem to be relevant to explain the low-frequency vibrational features below 350 cm^{-1} since they do not show clear activity in this region. Only the peak at 378 cm^{-1} for the γ -turn is explained by the out-of-plane motion of the free hydrogen atom of the NH_2 function. Sec-

4 CONCLUSIONS AND OUTLOOK

only, as the C7/C10 hydrogen bond leads to the folding of the peptide, we expect that both backbone motions and hydrogen bond motions are strongly coupled. This is indeed observed for the two conformers, as the hydrogen bond stretching signature and dihedral backbone motion signatures share common features in the ICDO spectra.

The spectra for the β - and γ -turns do not appear to be strongly conformer selective in the 240-400 cm^{-1} range. There are 7 peaks in common between the two spectra, deviating in position by only 2-14 cm^{-1} . Despite these similarities in the IR signatures, the assignments of the bands are surprisingly rather different. Although the intrinsic nature of the motions is similar, namely backbone motions, the coupling between these motions is different due to the two different backbone 3D folded structures in the γ - and β -turns. For instance, the 306/308 cm^{-1} peak, respectively for the γ - and β -turn, does not arise from the same motion. The former is related to the Φ_{Pro} torsional motion, while the latter comes from Φ_{Phe} torsion. Also, the two peaks located at 378 cm^{-1} for the γ -turn and 386 cm^{-1} for the β -turn are explained by different motions: out-of-plane motion of the NH_2 free hydrogen atom for the γ -turn, and coupled ω_{Pro} and Ψ_{Phe} motions for the β -turn. Of special interest are the two peaks (experiments and dynamical spectra) recorded in the 250-300 cm^{-1} domain, that carry γ - versus β -turn selectivity. They respectively differ by +17 and +14 cm^{-1} (from lower to higher frequency), going from γ - to β -conformer spectra: these two peaks are due to the amide peptide backbone motions namely Φ_{Pro} (lower frequency) and Φ_{Phe} (higher frequency). These backbone motions are direct probes of the C7/C10 folding of PhePro, thus providing conformer specific spectral signatures.

Although the H-bond strength is clearly reflected by the peak position for the γ - and β -turn conformers, the band pattern for the C7/C10 H-bond is very similar below 200 cm^{-1} . The H-bond signatures dominate the spectral assignments together with couplings to backbone torsions which are directly involved in the H-Bond motions. There are four dominant bands related to this H-Bond motion in the far-IR part of the spectra, respectively located at 115 cm^{-1} , 140 cm^{-1} , 163 cm^{-1} and 174 cm^{-1} in the BOMD spectrum of the γ -turn and 111 cm^{-1} , 143 cm^{-1} , 148 cm^{-1} and 175 cm^{-1} for the β -turn.

4 Conclusions and outlook

In this work, far-IR spectroscopy is shown to be a relevant tool for the characterization of peptide structures, since the observed far-IR features are a direct result from peptide backbone motions and hydrogen bond vibrations, and thereby directly reflect the secondary structure of peptides. The relationship between the delocalized backbone motions and the functional flexibility/rigidity of peptides and proteins can thus

be probed with this approach.

The experimental spectra reported here for two conformers of the Ac-Phe-Pro- NH_2 peptide, show very well-defined and well-resolved peaks from 800 down to 120 cm^{-1} . To fully exploit the far-IR region and to retrieve the structural information hidden in this region, reliable calculations are key. The presented combination of conformation selective far-IR/UV double resonance spectroscopy with Born Oppenheimer Molecular Dynamics simulations brings this synergy.

The present work is a follow-up on our previous initial demonstration²¹ that such synergy was indeed able to differentiate the axial and equatorial forms of the γ -turn interaction in Ac-Phe-Gly- NH_2 , which was not possible with mid-IR spectroscopy and harmonic DFT calculations^{22,23}. Here, we have investigated two different turns in the conformation of Ac-Phe-Pro- NH_2 , i.e. γ - (C7 H-Bond interaction) and β -turns (C10 H-Bond interaction), and have highlighted their specific far-IR signatures.

Clearly, the BOMD dynamical spectrum of the γ -turn conformation of Ac-Phe-Pro- NH_2 provides a better agreement with the experiment than the dynamical spectrum of the β -turn. This is especially true below 350 cm^{-1} where the H-Bond signatures are present. One reason might be the use of the GGA/BLYP functional (although augmented here by D3 van der Waals interactions), known to underestimate the strength of H-Bonds, and thus allowing too large amplitude motions of the hydrogen atoms involved in H-Bonds. One has also to keep in mind that nuclei quantum effects, especially of relevance to hydrogen atom motions, have not been taken into account in the present simulations. Such effects might help reduce some of the band-breadths, observed for H-Bonded motions of the β -turn conformer.

One main purpose of the combined experiment/BOMD spectra simulations was to provide conformer selective IR signatures of the γ - versus β -turns in the far-IR region. We have shown that the 400-550 cm^{-1} domain indeed provides such a distinction between the two conformers. This domain is predominantly due to N-H motions, indirectly probing the N-H...O H-bond motion. We have shown that there is a 29-38 cm^{-1} downshift in the positions of the associated bands for the weaker C7 interaction in the γ -turn conformer with respect to the C10 interaction in the β -turn.

The 800-550 cm^{-1} spectral domain was shown not to be conformer selective as bands in both conformers have very similar positions and same assignments from out-of-plane H atoms motions of the Phenyl ring and Pro residue, not sensitive to the γ/β turns. Also the backbone torsional domain in the 250-400 cm^{-1} does not provide too much conformer selectivity. Only the 250-300 cm^{-1} peaks carry γ - versus β -turn selectivity, as they respectively differ by +17 and +14 cm^{-1} (from lower to higher frequency) from the γ - to the β -conformer. These two signatures are due to the amide

REFERENCES

REFERENCES

peptide backbone motions, namely Φ_{Pro} (lower frequency) and Φ_{Phe} (higher frequency), which are direct probes of the C7/C10 folding of PhePro. The supplementary H-Bond signatures below 350 cm^{-1} have been shown to be of limited use for conformer selectivity.

Comparing the results of the γ -turn conformer of PhePro presented here with our previously published results on PheGly and PheAla γ -turns²¹, one worth comment concerns the H-bond length and its signature within the three systems. This H-Bond length is substantially shorter in PhePro (2.01 Å for the γ -turn and 1.95 Å for the β -turn) than in PheGly (2.14 Å) and PheAla (2.12 Å). As a result, this leads to higher frequencies associated with the H-bond stretching vibration for PhePro (140-150 cm^{-1} domain) than for PheGly and PheAla ($\sim 130\text{ cm}^{-1}$ domain). Probably due to the stronger H-bond strength, the H-bond stretching vibration then couples more strongly to backbone torsional vibrations, as can be seen from the hydrogen bond stretching activity at higher frequencies (e.g. 380 cm^{-1}) in the γ -turn of PhePro. In PheGly and PheAla, those bands were not observed.

Acknowledgement Computational resources were provided by support from HPC resources from GENCI-France (Grant 2012-2014 [072484]). This work is part of the research programme of the Stichting voor Fundamenteel Onderzoek der Materie (FOM), which is financially supported by the Nederlandse Organisatie voor Wetenschappelijk Onderzoek (NWO). Part of the FELIX laboratory is financed through the NWO BIG-programme. The calculations were sponsored by NWO Physical Sciences (EW) for the use of the supercomputer facilities at SurfSara. We also want to acknowledge Prof Michel Mons for providing the initial structure for the β -turn and for very fruitful discussions. We also acknowledge the very helpful comments from the reviewers, which significantly improved the quality of this paper.

References

- D. Kennedy and C. Norman, *Science*, 2005, **309**, 75.
- M. S. de Vries and P. Hobza, *Annu. Rev. Phys. Chem.*, 2007, **58**, 585–612.
- S. Jaeqx, J. Oomens and A. M. Rijs, *Phys. Chem. Chem. Phys.*, 2013, **15**, 16341–16352.
- R. J. Plowright, E. Gloaguen and M. Mons, *ChemPhysChem*, 2011, **12**, 1889–1899.
- K. Schwing, H. Fricke, K. Bartl, J. Polkowska, T. Schrader and M. Gerhards, *Chemphyschem*, 2012, **13**, 1576–1582.
- I. Hunig and K. Kleinermanns, *Phys. Chem. Chem. Phys.*, 2004, **6**, 2650–2658.
- M. Cirtog, A. M. Rijs, Y. Loquais, V. Brenner, B. Tardivel, E. Gloaguen and M. Mons, *J. Phys. Chem. Lett.*, 2012, **3**, 3307–3311.
- J. M. Bakker, L. M. Aleese, G. Meijer and G. von Helden, *Phys. Rev. Lett.*, 2003, **91**, 203003.
- P. Carcabal, R. T. Kroemer, L. C. Snoek, J. P. Simons, J. M. Bakker, I. Compagnon, G. Meijer and G. v. Helden, *Phys. Chem. Chem. Phys.*, 2004, **6**, 4546–4552.
- D. F. Plusquellic, K. Siegrist, E. J. Heilweil and O. Esenturk, *ChemPhysChem*, 2007, **8**, 2412–2431.
- R. Singh, D. K. George, J. B. Benedict, T. M. Korter and A. G. Markelz, *J. Phys. Chem. A*, 2012, **116**, 10359–10364.
- A. G. Markelz, *IEEE J. Sel. Top. Quantum Electron.*, 2008, **14**, 180–190.
- G. Acbas, K. A. Niessen, E. H. Snell and A. G. Markelz, *Nature Communications*, 2014, **36**, year.
- R. J. Falconer and A. G. Markelz, *J. Infrared Milli. Terahz. Waves*, 2012, **33**, 973–988.
- K. Itoh and T. Shimanouchi, *Biopolymers*, 1967, **5**, 921–930.
- R. Langner and G. Zundel, *J. Chem. Soc., Faraday Trans.*, 1995, **91**, 3831–3838.
- P. Godlewska, J. Jańczak, E. Kucharska, J. Hanuza, J. Lorenc, J. Michalski, L. Dymińska and Z. Węgliński, *Spectrochim. Acta Mol. Biomol. Spectros.*, 2014, **120**, 304–313.
- A. Abo-Riziq, L. Grace, B. Crews, M. P. Callahan, T. van Mourik and M. S. de Vries, *J. Phys. Chem. A*, 2011, **115**, 6077–6087.
- A. M. Rijs, M. Kabelac, A. Abo-Riziq, P. Hobza and M. S. de Vries, *ChemPhysChem*, 2011, **12**, 1816–1821.
- D. Oepts, A. F. G. van der Meer and P. W. van Amersfoort, *Infrared Phys. Technol.*, 1995, **36**, 297–308.
- S. Jaeqx, J. Oomens, A. Cimas, M. P. Gaigeot and A. M. Rijs, *Angew. Chem. Int. Ed.*, 2014, **53**, 3663–3666.
- W. Chin, F. Piuze, J. P. Dognon, I. Dimicoli and M. Mons, *J. Chem. Phys.*, 2005, **123**, 084301.
- W. Chin, J. P. Dognon, F. Piuze, B. Tardivel, I. Dimicoli and M. Mons, *J. Am. Chem. Soc.*, 2005, **127**, 707–712.
- V. Nibali and M. Havenith, *J. Am. Chem. Soc.*, 2014, **136**, 12800.
- J. Sun, G. Niehues, H. Forbert, D. Decka, G. Schwaab, D. Marx and M. Havenith, *J. Am. Chem. Soc.*, 2014, **136**, 5031.
- T. Luong, P. Verma, R. Mitra and M. Havenith, *Biophys. J.*, 2011, **101**, 925.
- N. Heine and K. Asmis, *Int. Reviews in Phys. Chem.*, 2015, **34**, 1.
- J. Bowlan, D. J. Harding, J. Jalink, A. Kirilyuk, G. Meijer and A. Fielicke, *J. Chem. Phys.*, 2013, **138**, 031102.
- W. Chin, M. Mons, J. P. Dognon, B. Piuze, F. Tardivel and D. I., *Phys. Chem. Chem. Phys.*, 2004, **6**, 2700–2709.
- A. M. Rijs and J. Oomens, *Top Curr Chem*, 2015, 4546–4552.
- M. V. Johnston, *Trends Anal. Chem.*, 1984, **3**, 58–61.
- J. VandeVondele, M. Krack, F. Mohamed, M. Parrinello, T. Chassaing and J. Hutter, *Comput. Phys. Comm.*, 2005, **167**, 103.
- The CP2K developers group, <http://www.cp2k.org/>, 2013.
- M. Krack, *Theor. Chem. Acc.*, 2005, **114**, 145.
- S. Goedecker, M. Teter and J. Hutter, *Phys. Rev. B.*, 1996, **54**, 1703.
- C. Hartwigsen, S. Goedecker and J. Hutter, *Phys. Rev. B.*, 1998, **58**, 3641.
- A. Becke, *Phys. Rev. A.*, 1988, **38**, 3098.
- C. Lee, W. Yang and R. G. Parr, *Phys. Rev. B*, 1988, **37**, 785.
- S. Grimme, J. Antony, S. Ehrlich and H. Krieg, *J. Chem. Phys.*, 2010, **132**, 154104.
- D. McQuarrie, *Statistical Mechanics*, Harper-Collins Publishers: New York, 1976.
- R. Kubo, M. Toda and N. Hashitsume, *Statistical Physics*, Springer Verlag, 2nd edn., 1991, vol. II.
- M. P. Gaigeot and M. Sprik, *J. Phys. Chem. B.*, 2003, **107**, 10344.
- R. Iftimie and M. E. Tuckerman, *J. Chem. Phys.*, 2005, **122**, 214508.
- H. Ahlborn, B. Space and P. B. Moore, *J. Chem. Phys.*, 2000, **112**, 8083.
- J. Borysow, M. Moraldi and L. Frommhold, *Mol. Phys.*, 1985, **56**, 913.
- R. Ramirez, T. Lopez-Ciudad, P. Kumar and D. Marx, *J. Chem. Phys.*, 2004, **121**, 3973.
- C. P. Lawrence and J. L. Skinner, 2005, **102**, 6720.
- H. Kim and P. J. Rossky, *J. Chem. Phys.*, 2006, **125**, 074107.

REFERENCES

REFERENCES

- 49 M. P. Gaigeot, *Phys. Chem. Chem. Phys.*, 2010, **12**, 3336.
- 50 C. Marinica, G. Grgoire, C. Desfranois, J. P. Schermann, D. Borgis and M. P. Gaigeot, *J. Phys. Chem. A.*, 2006, **110**, 8802.
- 51 A. Cimas, T. D. Vaden, T. S. J. A. de Boer, L. C. Snoek and M. P. Gaigeot, *J. Chem. Theor. Comput.*, 2009, **5**, 1068.
- 52 A. Cimas, P. Maitre, G. Ohanessian and M. P. Gaigeot, *J. Chem. Theor. Comput.*, 2009, **5**, 2388.
- 53 A. Sediki, L. C. Snoek and M.-P. Gaigeot, *Int. J. Mass Spectrom.*, 2011, **308**, 281.
- 54 J. P. Beck, M.-P. Gaigeot and J. M. Lisy, *Phys. Chem. Chem. Phys.*, 2013, **15**, 16736.
- 55 M. P. Gaigeot, R. Vuilleumier, M. Sprik and D. Borgis, *J. Chem. Theor. Comput.*, 2005, **1**, 772.
- 56 J. W. Handgraaf, E. J. Meijer and M. P. Gaigeot, *J. Chem. Phys.*, 2004, **121**, 10111–10119.
- 57 M. P. Gaigeot, *Phys. Chem. Chem. Phys.*, 2010, **12**, 10198.
- 58 D. Bovi, A. Mezzetti, R. Vuilleumier, M.-P. Gaigeot, B. Chazallon, R. Spezia and L. Guidoni, *Phys. Chem. Chem. Phys.*, 2011, **13**, 20954.
- 59 M. Sulpizi, M. Gaigeot and M. Sprik, *J. Chem. Theor. Comput.*, 2012, **8**, 1037.
- 60 M.-P. Gaigeot, M. Sprik and M. Sulpizi, *J. Phys.: Condens. Matter*, 2012, **24**, 124106.
- 61 M. Sulpizi, M. Salanne, M. Sprik and M. Gaigeot, *J. Phys. Chem. Letters*, 2013, **4**, 83.
- 62 B. Yan, S. Jaeqx, W. J. van der Zande and R. A. M., *Phys. Chem. Chem. Phys.*, 2014, **16**, 10770–10778.